

Thermal decomposition of ammonium nitrate modeling of thermal dissociation in thermal analysis

Koji Fujisato^{*†}, Hiroto Habu^{**}, Atsumi Miyake^{***}, and Keiichi Hori^{**}

^{*}Department of Chemical System Engineering, School of Engineering, the University of Tokyo,
7-3-1 Hongo, Bunkyo-ku, Tokyo 113-8656, JAPAN
Phone: +81-42-759-8481

[†]Corresponding address: fujisato.kohji@ac.jaxa.jp

^{**}Institute of Space and Astronautical Science/Japan Aerospace Exploration Agency
3-1-1 Yoshinodai, Sagami-hara, Kanagawa 229-8510, JAPAN

^{***}Graduate School of Environment and Information Sciences, Yokohama National University,
79-7, Tokiwadai, Hodogaya-ku, Yokohama 240-8501, JAPAN

Received: June 28, 2013 Accepted: August 30, 2013

Abstract

Pressure thermogravimetric-differential thermal analysis is used to study the thermal decomposition of ammonium nitrate (AN) in open and nonisothermal conditions as functions of the sample amount, heating rate, flow rate of purge gas, shape of sample pans, and pressure. The thermal decompositions are simulated using a physicochemical model. The thermal decomposition of AN consists of a chemical reaction and a thermal dissociation process—a physical process. The model considers thermal dissociation as a first-order diffusion model and succeeds in reproducing the experimental results. This method can be widely used for the thermal analysis of energetic materials.

Keywords: ammonium nitrate, thermogravimetric analysis, differential thermal analysis, thermal dissociation, thermal decomposition

1. Introduction

Ammonium nitrate (AN) is an important constituent of pyrotechnics and fertilizers and is used as an oxidizer in gas generators and propellants because it is inexpensive and environment friendly. In recent years, many researchers investigating green propellants have attempted to substitute AN in place of ammonium perchlorate (AP)—a common oxidizer in rocket motors.

Decomposition and combustion behaviors of AN have already been reported^{1,2}. However, practical applications of AN are difficult as AN-based propellants and gas generators have high-pressure deflagration limits (PDLs) in addition to high hygroscopicity and phase transitions. Thus, it is necessary to solve these problems through understanding AN decomposition mechanism.

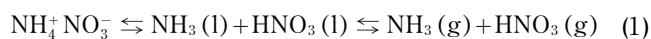
1.1 Decomposition mechanism of AN

The melting point of AN is 442 K, and its thermal

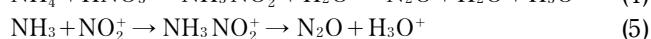
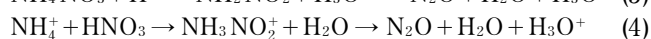
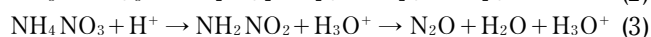
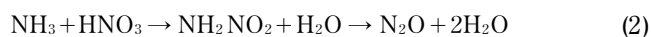
dissociation and chemical reactions start simultaneously. An older study shows that the heating of AN yields NH₃, and an acid remains in the liquid phase⁴. This decomposition is known as the thermal dissociation and is reversible and endothermic, as shown in Equation (1)⁵⁻⁷. On the other hand, the chemical reaction in the liquid phase proceeds irreversibly and exothermally. This is attributed to the nitration of amine, and it mainly produces N₂O and H₂O. The mechanism has been revealed via isotope studies⁸⁻¹⁰, based on which Equation (2)⁸, (3)¹¹, (4)¹², and (5)^{3,13} have been proposed. Equation (3) is based on the experiments conducted using acid catalysts. In Equation (5), NO₂⁺ is produced by dehydration and self-dissociation of HNO₃. All equations proceed via two dehydration steps: first, dehydration from AN or HNO₃, and second, dehydration from nitroamide caused by intermolecular hydrogen transfer. Many researchers have pointed out that the first dehydration process determines

the reaction rate¹¹⁻¹⁴. In addition to the main reaction, subreactions that mainly generate N₂, H₂O, and HNO₃ have been reported^{12,13}. The subreactions accounts for only a small percentage of the total chemical reactions at temperatures higher than 500 K; however, it forms a considerable percentage of the reactions at lower temperatures¹²⁻¹⁴.

Thermal dissociation of AN



Reaction of AN in liquid phase



High-temperature reaction kinetics involving gas-phase reactions is necessary for rapid phenomena such as combustion. Russel et al. measured the gas composition of AN decomposition using rapid-scan FT-IR at a high heating rate²⁵. At first, the evolved gas mainly consisted of NH₃ (g) and HNO₃ (g) at 600 K; gradually the N₂O (g) and NO₂ (g) content increased with an increase in the temperature. Measurable NH₃ (g) was observed even at 900 K; however, HNO₃ (g) rapidly decreased and became negligible at 800K, whereas NO₂ (g) content increased. Musin et al. calculated the reactions between NH₃ (g) and HNO₃ (g) with ab initio molecular orbital calculations and revealed that there are two reaction channels producing H₂NNO₂ (g) and H₂NONO (g) as the intermediates²⁶.

It is well known that the AN-decomposition temperatures decrease on the addition of either chloride or chromium¹⁵. Keenan et al. reported on synergistic catalytic effect of chloride and metals that can form chloro-complexes¹⁶. It is also known that carbon black enhances the AN decomposition¹⁸. Lurie et al. reported that carbon black reduces HNO₃ to HNO₂, which strongly accelerates the oxidation of NH₃ and NH₄⁺¹⁹. Levchenko et al. studied the effects of phase stabilizers to obtain phase-stabilized

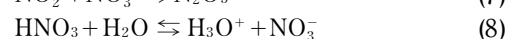
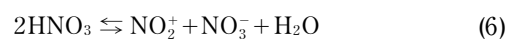
AN with minimum activation energy²⁰. Rubtsov et al. studied the effect of other additives such as guanidinium nitrate, pyroxylin, and organic acids, and revealed the kinetic regularities²¹⁻²⁴.

1.2 Difficulties in decomposition studies of AN

There are still difficulties in completely elucidating the AN-decomposition mechanism. Following are three reasons that complicate the experiments and analyses:

1. Some evaporative decomposition products affect the decomposition mechanisms. It is known that HNO₃ enhances the AN decomposition, whereas NH₃ and H₂O retard the same^{3,11,12}. Rosser et al. explained this phenomenon by Equations (1) and (7)³. In particular, the influence of HNO₃ is complicated because of the reversible equilibriums in liquid phase, as shown in Equation (6)–(8)²⁷. Thus, it is difficult to accurately calculate the reactant concentrations and reaction rate. In addition, Manelis et al. pointed that N₂O₅ causes subreactions.

Equilibrium of HNO₃ in liquid phase



2. Experiments in closed conditions face certain problems. It is difficult to control or calculate the reactant concentrations. For example, NH₃ is more volatile than HNO₃; as a result, HNO₃ accumulates in liquid phase as the decomposition progresses. Manelis et al. reported initial self-accelerated decomposition and dependencies on the free-volume caused by HNO₃ accumulation¹². In addition, it is difficult to separate the condensed and gas-phase reaction contributions to the results, and therefore the analysis becomes complex.

3. In open condition, it is easy to maintain the low concentration of HNO₃ in the liquid phase, and the reactions become simple. However, thermal dissociation (Equation (1)) and chemical reactions (Equation (2)–(5)) occur simultaneously, making it difficult to calculate the

Nomenclature		<i>Mass</i> mass change in thermogravimetric analysis	
<i>A</i>	Arrhenius frequency factor	<i>N_A</i>	thermal dissociation gas flux of ammonium nitrate
<i>A_{app}</i>	apparent Arrhenius frequency factor	<i>N_B</i>	decomposition gas flux of ammonium nitrate
<i>C_{sur}</i>	concentration of dissociated gas on the surface of condensed phase	<i>P</i>	total pressure
<i>C_{ex}</i>	concentration of dissociated gas on at the exit of sample pan	<i>p_{sat}</i>	saturated vapor pressure of the dissociated gas of ammonium nitrate
<i>d</i>	diameter of sample pan	<i>Q</i>	simulated heat value
<i>δ</i>	distance between condensed phase surface and exit of sample pan	<i>R</i>	universal gas constant
<i>D_{ab}</i>	inter diffusion coefficient of dissociated gases into purge gas	<i>ρ</i>	density
<i>E_a</i>	activation energy	<i>S</i>	bottom area of sample pan
<i>E_{app}</i>	apparent activation energy	<i>T</i>	temperature
<i>G</i>	flow rate of purge gas	<i>dT/dt</i>	heating rate
<i>h</i>	height of sample pan	<i>ΔT</i>	heat value measured by differential thermal analysis
<i>k</i>	reaction rate constant	<i>x_A</i>	partial pressure of dissociated gas on the surface of condensed phase
<i>M</i>	mass of sample		

reaction parameters. Thermal dissociation is a physical process expressed by vapor pressure equation, and the chemical process is expressed by Arrhenius' equation. It is necessary to calculate the contributions separately; however, the calculation method of thermal dissociation rate has not been established in thermal analysis. Thus, if it is possible to evaluate the thermal dissociation rate, open condition is better than the closed one for the study of AN decomposition.

In this report, we propose a simple thermal dissociation model for a general thermal analysis and try to understand the thermal decomposition mechanism of AN. The mechanisms of thermal dissociation and chemical reaction have been considered, and their validity and applicability for high energetic materials are also discussed. The thermal dissociation rate is evaluated using a first-order diffusion model, and the reaction rate is calculated by Arrhenius' equation using the reported reaction parameters. The calculation considers all the experiments carried out under various conditions, including pressure change.

2. Thermal dissociation model

2.1 Conventional model

Some methods have been proposed to analyze the physical processes of thermal decompositions. Some thermal behaviors cannot be simulated by Arrhenius' equation, such as gas desorption, melting, crystallization, and glass transition, because they are physical processes. However, some of them can be formulated by apparent activation energy and apparent frequent factor, which is known as the kinetic compensation effect (KCE).

Analyses based on KCE can also be applied to the AN decomposition. Koga *et al.* studied the AN decomposition in an open condition and analyzed it by KCE^{28),29)}. According to them, considering A_{app} as $AS\rho/M$, A_{app} and the inverse of temperature can be plotted on a straight line, and the slope equals to E_{app} .

Vyazovkin *et al.* also studied AN decomposition in an open condition and applied the modified integral isoconversional method, which is based on KCE³⁰⁾. The integral isoconversional method was developed by Ozawa³¹⁾, and Flynn and Wall³²⁾ independently. It is generally used to calculate the reaction parameters. The modified method can calculate local activation energy at an arbitrary extent of the reaction³³⁾. It is necessary to choose the reaction model from the proposed equations to calculate the kinetic parameters. Vyazovkin *et al.* showed that the AN decomposition is described by the contract cylinder model, which means that the decomposition rate depends on the thermal dissociation rate.

However, these two methods cannot clarify the physicochemical mechanism as they are not suitable for the decomposition consisting of more than two phenomena. It was tried to elucidate the contributions of thermal dissociation and chemical reaction of AP, RDX (hexahydro-1,3,5-trinitro-1,3,5-triazine) and NTO (5-nitro-2,4-dihydro-3H-1,2,4-triazol-3-one)³⁴⁾⁻³⁶⁾. These reports showed that the decomposition consists of

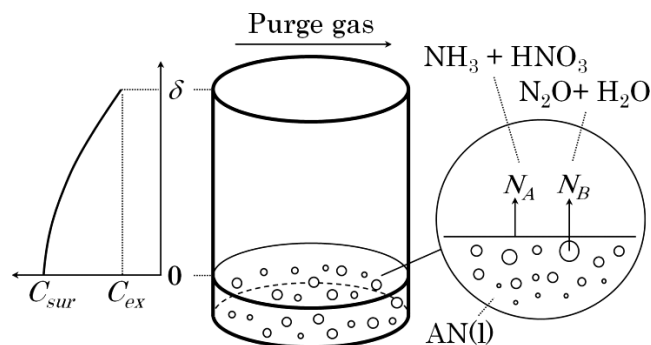


Figure 1 Sample pan configuration.

dissociation (or sublimation) and chemical reactions, and the contribution of dissociation is lower in the closed or pierced pans than in open pans. However, it seems difficult to quantitatively evaluate the contribution of the dissociation process because isoconversional method considering only one reaction model was used in those reports. Therefore, it is important to apply an appropriate physicochemical model to the thermal dissociation and chemical reactions in order to understand the decomposition mechanisms.

2.2 Our model

Figure 1 shows the configuration of a sample pan. The thermal dissociation gas flux of AN is shown as the unidirectional diffusion equations (Equation (9) and (10)).

The thermal dissociation gas flux of AN consists of NH_3 and HNO_3 . The dissociation flux is multiplied by the dissociation area to give the thermal dissociation rate. The decomposition gases, which mainly consist of N_2O and H_2O , generated by the chemical reactions shown in Equations (2)–(5). The decomposition gas flux is calculated as the Arrhenius-type reaction rate using the reported parameters.

$$N_A = D_{ab} \frac{(C_{sur} - C_{ex})}{\delta} + x_A (N_A + N_B) \quad (9)$$

$$D_{ab} \propto P^{-1}, T^{1.75} \quad (10)$$

D_{ab} is the interdiffusion coefficient of the dissociated gases—the mixture of NH_3 and HNO_3 —into purge gas. No experimental D_{ab} has been reported, and its value is assumed to be close to the averaged D_{ab} of the other gases, which is approximately $10^{-5} \text{ m}^2\text{s}^{-1}$ under the standard state. In general, D_{ab} is proportional to P^{-1} ³⁷⁾. D_{ab} is theoretically proportional to $T^{1.5}$ and experimentally $T^{1.75}$ ³⁸⁾. In this report, the experimental value was used as shown in Equation (10).

C_{sur} is assumed to be equivalent to p_{sat}/RT . C_{ex} is approximated by zero, because the purge gas flow rate is assumed to be sufficient to flow out the dissociated gas over the sample pan. Temperature changes during the measurement as the experiments are conducted under nonisothermal conditions. S is the dissociation area, and equals the area of the base of sample pans; x_A is the partial pressure of the dissociated gas on the surface of the condensed phase and is expressed as C_{sur}/P .

Table 1 Experimental condition at ambient pressure.

No.	1	2	3	4	5	6	7	8	9
P [MPa]	0.1	0.1	0.1	0.1	0.1	0.1	0.1	0.1	0.1
M [mg]	2.0	5.0	15.0	5.0	5.0	5.0	5.0	5.0	5.5
h [mm]	3.2	3.2	3.2	3.2	3.2	3.2	2.5	5.0	5.0
d [mm]	3.5	3.5	3.5	3.5	3.5	3.5	5.0	5.0	5.0
dT/dt [Kmin ⁻¹]	5.0	5.0	5.0	1.5	20.0	5.0	5.0	5.0	10.0
G [Lmin ⁻¹]	0.2	0.2	0.2	0.2	0.2	0.05	0.2	0.2	0.2

Table 2 Experimental conditions at high pressures.

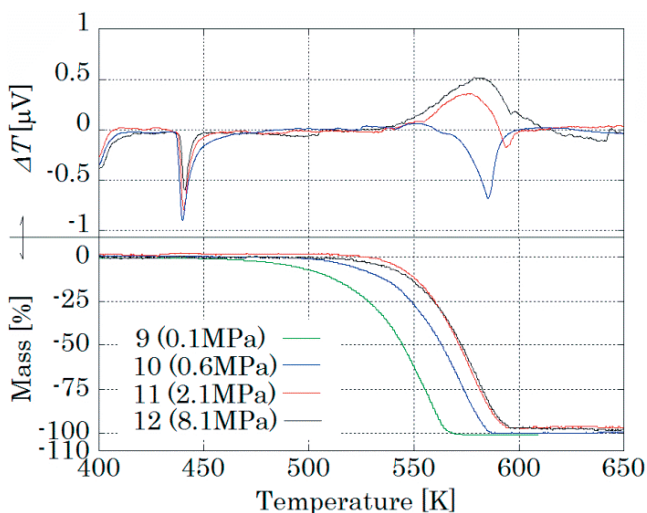
No.	10	11	12
P [MPa]	0.6	2.1	8.1
M [mg]	5.5	5.5	5.5
h [mm]	5.0	5.0	5.0
d [mm]	5.0	5.0	5.0
dT/dt [Kmin ⁻¹]	10.0	10.0	10.0
G [Lmin ⁻¹]	0.5	1	1

3. Experiments

Pressure thermogravimetric-differential thermal analysis (TG-DTA) is used to study the thermal decomposition of AN in the open condition. Tables 1 and 2 show the measurement conditions in the ambient and pressurized environments.

4. Results and discussion

Figure 2 shows the results of experiments; No.9–12. The DTA profile at 0.6 MPa (No. 10) corresponds to the endothermic reaction during the decomposition. This behavior turns into exothermic reaction at 2.1 MPa (No.11) in the range 540–590K and retains the endothermic profile at 590–600K. The result at 8.1 MPa (No. 12) corresponds to the exothermic decomposition (540–620 K); the peak is higher than that observed at 2.1 MPa. Based on the TGA measurements, the onset temperature of the decomposition becomes higher as the pressure increases up to 2.1 MPa; however, the TGA curves at 2.1 and 8.1 MPa are almost the same.

**Figure 2** Pressure TG-DTA results.

The comparisons of experiments and calculations are shown in the following subsections including the results under atmospheric pressure.

4.1 Calculation details

Thermal dissociation is shown in Equation (1), and the flux is calculated by Equation (9). It is necessary to know the saturated vapor pressure of the dissociated gas and D_{ab} . The saturated vapor pressure was measured by Brander et al., and it is expressed as Equation (11)⁶. The dissociation heat of AN is 166.9 kJmol⁻¹, which was measured under the ambient pressure in the range 343–523K. However, the dissociation heat is assumed to be constant, and thus the equation can be extended to higher pressure and higher temperatures. D_{ab} is fitted to experiments, and the value is 6×10^{-6} m²s⁻¹.

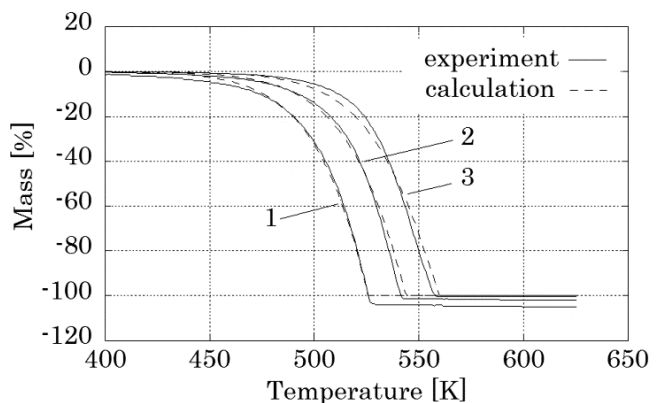
The rate of chemical reactions, Equation (2)–(5), is expressed by Equation (12), as obtained by Oxley et al. with differential scanning calorimetry (DSC) at the range 523–723 K; the reaction heat is 107 kJmol⁻¹²⁰. This equation is obtained in closed conditions, and thus, it is considered that this rate includes the accelerated reactions caused by the accumulated HNO₃.

$$\ln p_{sat} = 10040 - \frac{166900}{2RT} \quad (11)$$

$$\ln k = 8.81 - \frac{122000}{RT} \quad (12)$$

4.2 Initial sample amount

Figure 3 shows the effect of the initial sample amount on the TGA results. The solid lines denote the experiments, and dashed lines denote the simulations. The onset temperatures of the decompositions shift to higher temperatures as the sample amount increases. The

**Figure 3** Effects of sample amount.

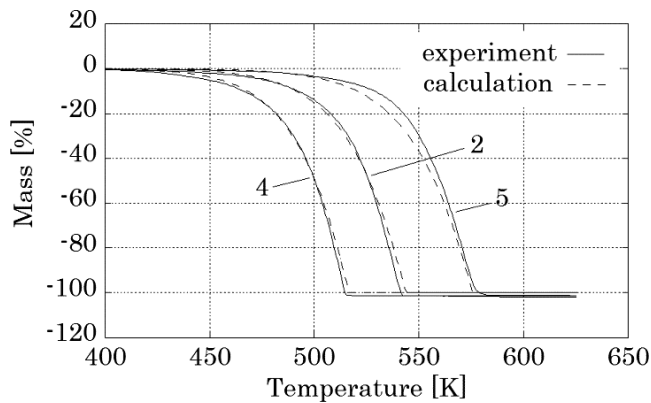


Figure 4 Effects of heating rate.

simulations are close to the experimental data. The ratio of the dissociated AN can be estimated by simulations and are 95% and 87% in experiment No.1 and 2, respectively. Therefore, most of the mass loss in these experiments is attributed to dissociation, and it is considered that Equation (9) can accurately estimate the dissociation contributions. The dissociation rate in the experiment No.3 is 69%; the reaction term is also accurately calculated.

4.3 Heating rate

Figure 4 shows the TGA measurements obtained using different heating rates. The onset temperatures of the decompositions increase as the heating rate increase. The contributions of thermal dissociations to total AN decompositions are 91%, 87%, and 81% in the order of the increasing heating rate. They all coincide well with the simulated curves, thus confirming that the dissociation and reaction rates are evaluated accurately.

4.4 Purge gas flow rate

When the flow rate changes from 0.2 Lmin^{-1} (No.2) to 0.05 Lmin^{-1} (No.6), the TGA profiles are almost same (Figure 5). It is obvious that the purge gas does not change the decomposition gas flow inside the sample pans. The dissociation rate equation, Equation (9), does not consider flow rates, and thus the results also support the validity of our model.

4.5 Shape of sample pan

Figure 6 shows the effect of the shape of sample pan in the TGA results, and the mass loss starts at lower

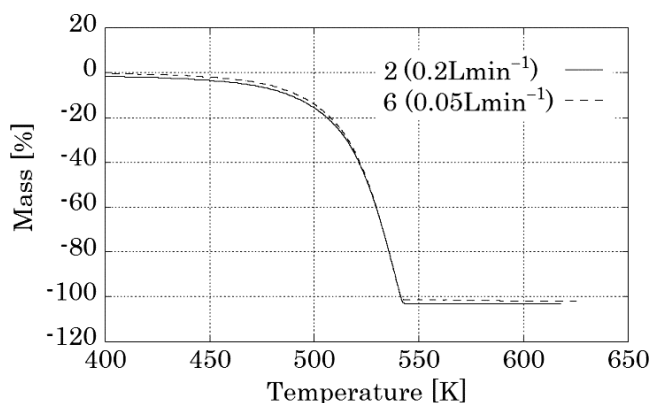


Figure 5 Effects of purge gas flow rate.

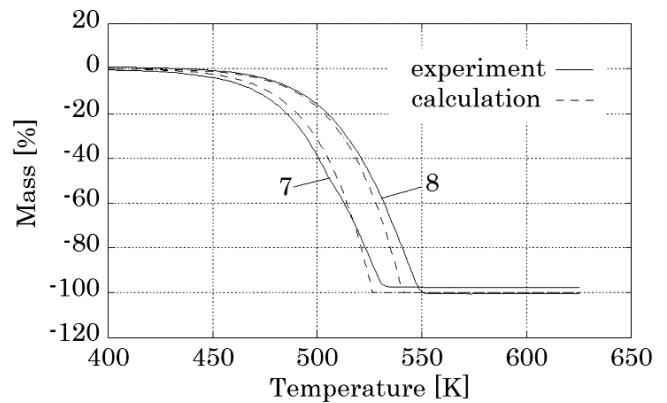


Figure 6 Effects of sample pan shape.

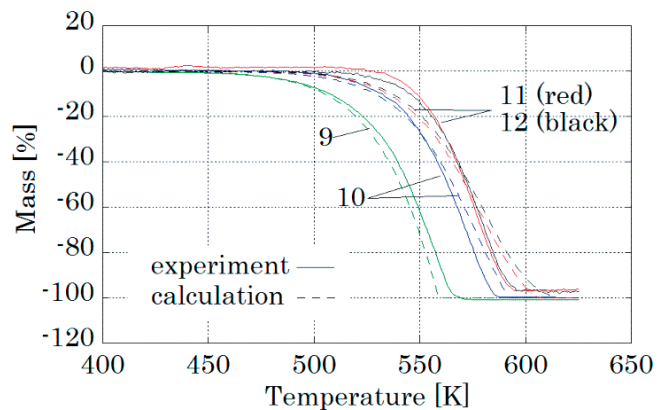


Figure 7 Effects of pressure change.

temperatures in a shallow pan compared to the deeper one. The results are well simulated, and the contributions of thermal dissociations are 95% and 89% in No.7 and 8, respectively. These experiments show that the diffusion controls the rate of dissociation in the sample pans.

4.6 Pressure

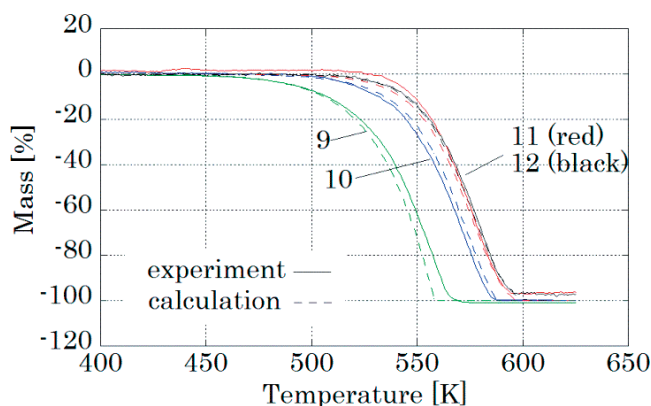
Figure 7 depicts the results of TGA at various pressures. The simulated TG curves coincide with the experiments at the ambient pressure; however, the TG curves show different tendencies at high pressures. The simulated mass-loss rates are slower than the experimental ones. The simulated TGA curves of 2.1 and 8.1 MPa are almost the same and the onset temperature is approximately 10K higher than that at 0.6 MPa, which is the same as observed in the experiments. However, the experimental curves show higher temperature dependencies than the simulated ones. It is necessary to modify the reaction or dissociation parameters to simulate these observations. Even if D_{ab} is modified, the temperature dependencies of the simulated mass-loss curves do not fit to the experiments. Thus, it is necessary to modify the reaction-rate parameters to simulate the experimental results.

4.7 Parameter modification and the decomposition mechanism

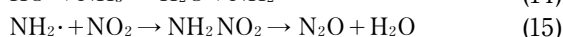
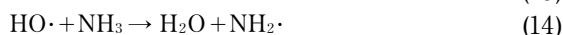
Brower et al. reported more accurate decomposition mechanism in addition to the DSC analysis. According to the report, the activation energy of AN gradually changed

Table 3 Parameters published and used in this report.

	A [s ⁻¹]	E _a [kJmol ⁻¹]	D _{ab} [m ² s ⁻¹]
High temperature (T>563K) ¹⁷⁾	10 ^{13.5}	175	–
Low temperature (T<563K) ¹⁷⁾	10 ^{6.09}	95.9	–
Overall (523<T<723K) ¹⁷⁾	10 ^{8.81}	122	–
Parameter A (Figures 3–7)	10 ^{8.81}	122	6.0×10 ⁻⁶
Parameter B (Figures 8,9)	10 ^{13.5}	171	6.5×10 ⁻⁶

**Figure 8** Calculation of TGA profiles with Parameter B in [Table3].

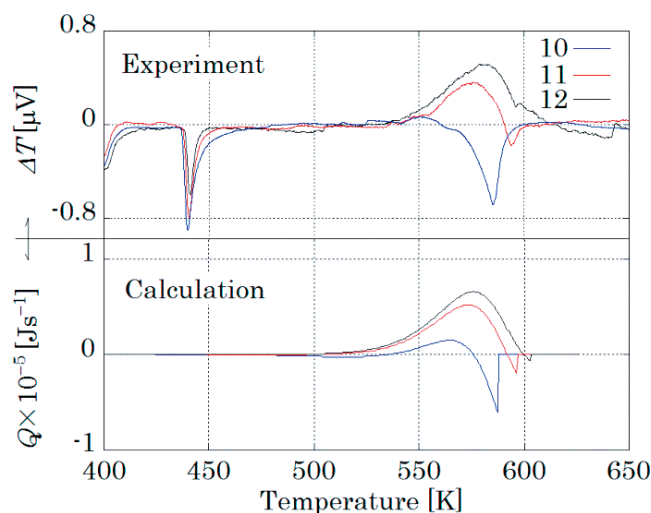
from 118 kJmol⁻¹ to 193 kJmol⁻¹ in the temperature range 470–650 K¹³⁾. They proposed that the radical reactions, Equation (13)–(15), overtake the ionic reaction, Equation (5). In other words, a slow reaction starting at a low temperature is overtaken by a fast reaction starting at a high temperature. Oxley et al. recommend $A = 10^{13.5} \text{ s}^{-1}$ and $E_a = 175 \text{ kJmol}^{-1}$ at temperatures higher than 563 K, and $A = 10^{6.09} \text{ s}^{-1}$ and $E_a = 95.9 \text{ kJmol}^{-1}$ at lower temperatures¹⁷⁾. The values of the reaction parameters used in Figures 3–6 lie intermediate of this range; $A = 10^{8.81} \text{ s}^{-1}$ and $E_a = 122 \text{ kJmol}^{-1}$.



It is necessary to replace the reaction parameters with fast reaction parameters for reactions at high temperature so as to accurately simulate the experiments. Thus, a new parameter, Parameter B, in Table 3 was used, based on the Oxley's parameter of high-temperature reaction. The frequency factor is same, and the activation energy is only 4kJmol⁻¹ lower than Oxley's one.

The TGA simulations are shown in Figure 8. The differences seen in Figure 7 between the simulation and experiments cannot be found in Figure 8. It is also confirmed that Parameter B can very well simulate the experimental results at ambient pressure, similar to Figures 3–6. Thus, it is considered that Parameter B is appropriate for our experimental results.

The DTA simulations by Parameter B are shown in Figure 9. The DTA values cannot be compared to the simulated ones because the units are different. However it is possible to compare each shape because it depends on the ratio of dissociation and reaction. The DTA result at 0.6 MPa has an endothermic peak at 580 K, and it is almost

**Figure 9** Calculation of DTA profiles with Parameter B [Table3].

the same in the experimental results. At 2.1 and 8.1 MPa, the DTA results have exothermic peaks at 570 and 580 K, respectively, which also agrees with the experiments. Thus, these agreements show that the ratio of dissociation and reaction are accurately calculated.

The parameters of the Oxley's low-temperature reaction, $A = 10^{6.09} \text{ s}^{-1}$ and $E_a = 95.9 \text{ kJmol}^{-1}$, are also tried. However, the mass-loss rates become slower in comparison to the simulation shown in Figure 7 and the error become bigger. Then, it is shown that Equations (8)–(10) are the main reactions and Equations (2)–(5) can be ignored under our experimental conditions.

Unlike the Oxley's experiments, the measurements were conducted in the open condition in this study. Thus, the reaction at low temperatures, Equations (2)–(5), occur only under the closed conditions, and some volatile substances start the reaction because they are accumulated in closed conditions. Volatile substances generated during the AN decomposition are HNO₃, H₂O, and NH₃. It is reported that HNO₃ accelerates and H₂O and NH₃ retard the AN decomposition. It is considered that HNO₃ enhances the Equations (2)–(5) in the closed conditions. On the other hand, volatile substances such as HNO₃ do not change the reaction rate of Equations (8)–(10) in both the open and closed conditions. Therefore, our experiments can be simulated with only thermal dissociation Equation (1) and the reaction at high temperatures, Equations (13)–(15).

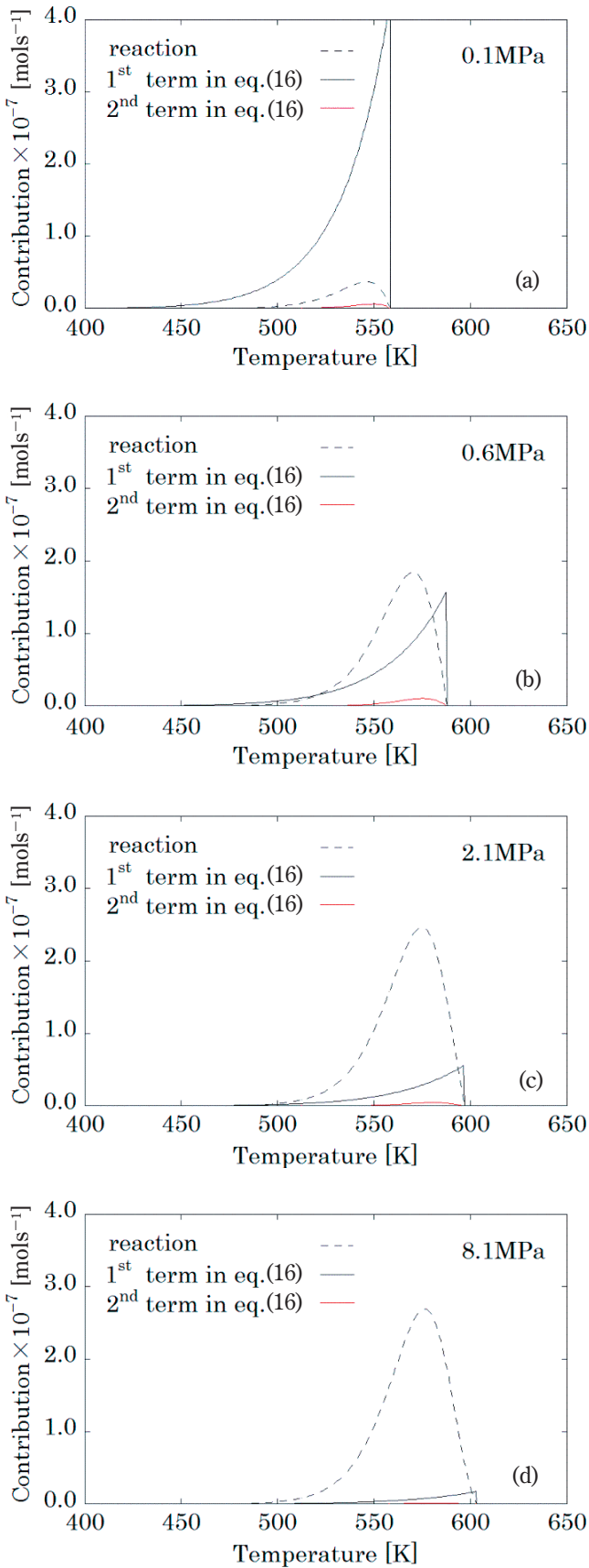


Figure 10 Contributions of Equation (17) and reaction.

4.8 Contributions of thermal dissociation and reactions

Figure 10 shows the calculated contributions of dissociation and reaction under various pressures. The dissociation and reaction parameters are the same as that

used in Figures 8 and 9. The dissociation gas flux of AN is expressed by Equation (16), reformulated from Equation (9); thus, the contribution is divided into two terms. The first term is the mass flux of AN derived from diffusion and convection caused by its own diffusion. The second term is the mass flux of AN derived from convection caused by the reaction gases, except for the AN dissociation gas. The contribution of the first term of Equation (16) becomes small as the pressure increases; as a result, the onset temperature of the decomposition shifts to high temperatures. Although the reaction rate is theoretically independent of pressure, it becomes the main contributor with increase in reaction temperature.

The second term in Equation (16) is proportional to the reaction gas flux and x_A . The reaction contribution become large and x_A become small as the pressure increases, and thus the contribution of the second term in Equation (16) become largest at 0.6 MPa (Figure 10–b). However, this contribution is only 2.4% of the total mass-loss even at 0.6 MPa, and therefore, we can simplify Equation (16) with Equation (17).

$$N_A = D_{ab} \frac{(C_{sur} - C_{ex})}{\delta (1 - x_A)} + \frac{x_A N_B}{(1 - x_A)} \quad (16)$$

$$\cong D_{ab} \frac{(C_{sur} - C_{ex})}{\delta (1 - x_A)} \quad (17)$$

4.9 Validity of our dissociation model

This thermal dissociation model includes assumptions; $C_{ex} = 0$, $C_{sur} = p_{sat}/RT$. If the reaction rate is much higher than that of thermal diffusion, C_{ex} cannot be assumed to be zero, and C_{sur} become smaller than p_{sat}/RT because C_{sur} is diluted by the reaction gas. However, it seems unnecessary to calculate N_A in such cases as the thermal dissociation becomes much smaller than N_B . In addition, δ does not equal the diffusion length in some conditions; the height of the sample pan is short, and the amount of the sample and the flow rate of the purge gas are large. In these cases, turbulence occurred inside the sample pan and the diffusion rate could not be calculated by Equation (9). If the purge gas flow rate is very small, C_{ex} does not equal zero as the dissociated gas partial pressure outside of the sample pan cannot be ignored. The dissociation model Equation (9) is not useful in the above conditions. However, these are not critical problems and can be avoided in ordinary thermal analysis by changing the settings. Thus, this dissociation model can be applied to many high energetic materials that decompose with dissociations and chemical reactions in the open condition.

Jacobs et al. the studied sublimation rate of AP^{39,40}, and the proposed formula is basically the same as for Equation (9). However, AP does not melt during decomposition. The attention was given to sublimation from the solid surface and thus the analysis was more complicate and specific than in Equation (9). Moreover, they used the evaporation coefficient in the equation. However, it is difficult to know the pressure and temperature dependencies of this value. Thus, it is difficult to apply it to other substances. In the case of AN, it melts before decomposition, and thus, it is

not necessary to discuss the specific phenomena. As a result, it was shown that the dissociation rate can be calculated by only one parameter, D_{ab} . In addition, this value is generally about $10^{-5} \text{ m}^2\text{s}^{-1}$ in most gases, and the dependencies on the temperature and pressure are known³⁸. Thus, both the dissociation rate and reaction rates could be discussed.

4.10 Summary of discussion

Thermal decomposition of AN was measured by TG-DTA in an open condition, and the results are simulated by a physicochemical model that consists of dissociation and reaction. When Oxley's parameters obtained by DSC are used, the simulation coincides with the experimental results at the ambient pressure; however, at high pressures, the gap becomes relatively large. Then, the parameters are replaced with Parameter B based on the Oxley's high-temperature reaction parameters. The simulations coincided with all the experiments, and thus, it was considered that the dissociation model is correct and the main chemical reactions are Equations (13)–(15). It is also shown that Equations (2)–(5) are enhanced by HNO_3 because the reaction can be ignored in open conditions. Each contribution of thermal dissociates and chemical reactions are also evaluated, and it is reported that the dissociation rate can be simplified to Equation (17) and this equation can be widely used.

5. Conclusion

Thermal decomposition of AN was studied with Pressure TG-DTA in open and nonisothermal conditions. The obtained results were well simulated by physicochemical model in varying conditions including pressure change. The model consisted of thermal dissociation and chemical reaction. The thermal dissociation rate was calculated using the unidirectional diffusion equation, and at first the accuracy was confirmed at ambient pressure. Next, the calculated pressure dependency of thermal dissociation rate also coincided with the pressurized experiments. Then, the reaction terms are discussed in detail and it was shown that this method can be widely used for thermal analysis of high energetic materials.

Acknowledgement

This work was funded by The Foundation for the Promotion of the Industrial Explosives Technology.

References

- 1) C. Oommen and S. R. Jain, *J. Hazard. Mater.*, A67, 253–281 (1999).
- 2) S. Chaturvedi and P. N. Dave, *J. Energ. Mater.*, 31, 1–26 (2013).
- 3) W. A. Rosser, S. H. Inami, and H. Wise, *J. Phys. Chem.*, 67, 1753–1757 (1963).
- 4) J. P. Emmet, *Am. J. Sci. Arts*, 18, 255–260 (1830).
- 5) M. Mozurkewich, *Atmos. Environ., Part A*, 27, 261–270 (1993).
- 6) J. D. Brandner, N. M. Junk, J. W. Lawrence, and J. Robins, *J. Chem. Eng. Data*, 7, 227–228 (1962).
- 7) G. Feick, *J. Am. Chem. Soc.*, 76, 5860–5863 (1954).
- 8) L. Friedman and J. Bigeleisen, *J. Chem. Phys.*, 18, 1325–1331 (1950).
- 9) W. S. Richardson and E. B. Wilson, *J. Chem. Phys.*, 18, 694–696 (1950).
- 10) J. T. Kummer, *J. Am. Chem. Soc.*, 69, 2559–2559 (1947).
- 11) B. J. Wood and H. Wise, *J. Chem. Phys.*, 23, 693–696 (1954).
- 12) G. B. Manelis, G. M. Nazin, Y. I. Rubtsov, and V. A. Strunin, "Thermal Decomposition and Combustion of Explosives and Propellants", 175, Taylor & Francis Inc. (2003).
- 13) K. R. Brower, J. C. Oxley, and M. Tewari, *J. Phys. Chem.*, 93, 4029–4033 (1989).
- 14) H. L. Saunders, *J. Chem. Soc.*, 121, 698–711 (1922).
- 15) A. G. Keenan, *J. Am. Chem. Soc.*, 77, 1379–1380 (1955).
- 16) A. G. Keenan, K. Notz, and N. B. Franco, *J. Am. Chem. Soc.*, 91, 3168–3178 (1969).
- 17) J. C. Oxley, S. M. Kaushik, and N. S. Gilson, *Thermochim. Acta*, 153, 269–286 (1989).
- 18) Y. Izato, A. Miyake, and S. Date, *Propellants, Explos., Pyrotech.*, 38, 129–135 (2013).
- 19) B. A. Lurie and C. Lianshen, *Combust., Explos. Shock Waves (Engl. Transl.)*, 36, 607–617 (2000).
- 20) I. V. Levchenko, G. F. Klyakin, I. A. Vyaznova, and V. A. Taranushich, *Russ. J. Appl. Chem.*, 84, 1511–1515 (2011).
- 21) A. I. Kazakov, Y. I. Rubtsov, D. B. Lempert, and G. B. Manelis, *Russ. J. Appl. Chem.*, 76, 1214–1220 (2003).
- 22) Y. I. Rubtsov, A. I. Kazakov, D. B. Lempert, and G. B. Manelis, *Russ. J. Appl. Chem.*, 77, 1083–1091 (2004).
- 23) Y. I. Rubtsov, A. I. Kazakov, E. P. Kirpichev, D. B. Lempert, and G. B. Manelis, *Russ. J. Appl. Chem.*, 78, 870–879 (2005).
- 24) Y. I. Rubtsov, A. I. Kazakov, D. B. Lempert, and G. B. Manelis, *Propellants, Explos., Pyrotech.*, 31, 421–434 (2006).
- 25) T. P. Russell and T. B. Brill, *Combust. Flame*, 76, 393–401 (1989).
- 26) R. N. Musin and M. C. Lin, *J. Phys. Chem. A*, 102, 1808–1814 (1998).
- 27) G. D. Robertson Jr., D. M. Mason, and W. H. Corcoran, *J. Phys. Chem.*, 59, 683–690 (1955).
- 28) N. Koga and H. Tanaka, *Thermochim. Acta*, 209, 127–134 (1992).
- 29) N. Koga and H. Tanaka, *Thermochim. Acta*, 240, 141–151 (1994).
- 30) S. Vyazovkin, J. S. Clawson, and C. A. Wight, *Chem. Mater.*, 13, 960–966 (2001).
- 31) T. Ozawa, *Bull. Chem. Soc. Jpn.*, 38, 1881–1886 (1965).
- 32) J. H. Flynn and L. A. Wall, *J. Polym. Sci.*, B4, 323–328 (1966).
- 33) S. Vyazovkin, *J. Comput. Chem.*, 18, 393–402 (1997).
- 34) G. T. Long, S. Vyazovkin, B. A. Brems, and C. A. Wight, *J. Phys. Chem. B*, 104, 2570–2574 (2000).
- 35) G. T. Long, B. A. Brems, and C. A. Wight, *J. Phys. Chem. B*, 106, 4022–4026 (2002).
- 36) A. J. Lang, S. Vyazovkin, *Combust. Flame*, 145, 779–790 (2006).
- 37) S. Chapman, *Philos. Trans. R. Soc. London, A*, 217, 115–197 (1918).
- 38) E. N. Fuller, P. D. Schettler, and J. C. Giddings, *Ind. Eng. Chem.*, 58, 18–27 (1966).
- 39) P. W. Jacobs and A. Russell-Jones, *J. Phys. Chem.*, 72, 202–207 (1968).
- 40) C. Guirao and F. A. Williams, *J. Phys. Chem.*, 73, 4302–4311 (1969).

硝酸アンモニウムの熱分解 熱分析における熱解離のモデル化

藤里公司*†, 羽生宏人**, 三宅淳巳***, 堀恵一**

高圧示差熱天秤を用い、硝酸アンモニウム (AN) の熱分解挙動を研究した。実験は全て非等温開放系で行い、試料量、昇温速度、パージガス流量、サンプルパン形状、圧力の影響を調べた。これらの熱分解挙動を物理化学モデルによりシミュレーションした。ANの熱分解は化学反応と物理変化のひとつである熱解離を伴う。熱解離速度を一次元拡散モデルにより計算することで、実験結果を再現することができた。本手法は汎用性が高く、他のエネルギー物質の熱分析にも適用できる。

*東京大学大学院工学系研究科化学システム工学専攻 〒113-8656 東京都文京区本郷7-3-1
Phone: 042-759-8481

† Corresponding address: fujisato.kohji@ac.jaxa.jp

**宇宙航空研究開発機構宇宙科学研究所 〒252-5210 神奈川県相模原市中央区由野台3-1-1

***横浜国立大学大学院環境情報研究院 〒240-8501 横浜市保土ヶ谷区常盤台79-7